FINAL REPORT

# CHARGED PARTICLE RADIATION DAMAGE IN SEMICONDUCTORS, IX:

## PROTON RADIATION DAMAGE

## IN SILICON SOLAR CELLS

8653-6024-KU-000

21 AUGUST 1963

SPACE TECHNOLOGY LABORATORIES, INC.
REDONDO BEACH, CALIFORNIA

FINAL REPORT

# CHARGED PARTICLE RADIATION DAMAGE IN SEMICONDUCTORS, IX:

# PROTON RADIATION DAMAGE

# IN SILICON SOLAR CELLS

CHARGED PARTICLE RADIATION DAMAGE IN SEMICONDUCTORS, IX:

PROTON RADIATION DAMAGE IN SILICON SOLAR CELLS

By
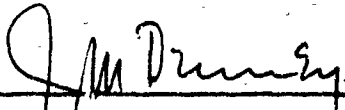
J. M. Denney
R. G. Downing

MR-34
31 August 1963

8653-6026-KU-000

Contract No. NAS5-1851

Solid State Physics Laboratory

Approved: _____

Joseph M. Denney, Director
Solid State Physics Laboratory

SPACE TECHNOLOGY LABORATORIES, INC.
One Space Park
Redondo Beach, California

## ABSTRACT

*18050*

A series of experiments using protons of energies from 6.7 Mev to 26 Mev were performed to measure the energy dependence of proton radiation damage on p on n and n on p silicon and gallium arsenide solar cells. The experimental results indicate that: (a) the energy dependence experimentally observed in this energy range is in agreement with the inverse energy dependence predicted on the basis of Coulomb scattering and (b) the minority carrier diffusion length injection level dependence previously observed at 95.5 Mev is also observed at all the energies used in this series of experiments. The energy dependence is presented for solar cells under one sun equivalent radiation in terms of both K values and reciprocal critical fluxes.

*Author* ⟶

ACKNOWLEDGMENT

TABLE OF CONTENTS

LIST OF ILLUSTRATIONS

## LIST OF ILLUSTRATIONS CON'T

## I.    INTRODUCTION

The existence of intense regions of energetic proton radiation in space
has stimulated considerable interest in the effects of proton radiation on
semiconductor devices during the last several years. Primary attention has been
directed in these efforts to silicon and silicon solar cells because of their
necessarily high degree of exposure to proton radiation when mounted on the exterior
of spacecraft. Semiconductor devices located in the interior of spacecraft,
though equally as sensitive to proton radiation, are afforded considerable
shielding from the satellite structure itself and hence may not constitute as
severe a problem as solar cells.

The dependence of proton radiation damage on proton energy is an important
factor because of the wide energy distribution of protons in space and the strong
dependence of radiation damage on incident proton energy. Protons of a few
hundred electron volts possess sufficient momentum to produce lattice displace-
ments and subsequent degradation of electrical characteristics in silicon. However,
the range of protons of energies less than an Mev is quite short and hence penetra-
tion at these energies is insufficient to produce meaningful radiation damage in
covered solar cells. As the proton energy increases, however, the proton range
increases resulting in a practical energy dependence of proton radiation damage
which increases sharply with increasing proton energy. In the medium energy range,
i.e., a few Mev, to approximately 100 Mev the proton range is quite large relative
to device geometries, and the resulting energy dependence of the radiation damage
follows the classical Coulomb scattering laws. These theoretical relationships
predict an energy dependence based on the atomic displacement cross section which
is inversely proportional to the incident proton energy. Extrapolation of this
energy dependence to proton energies above 100 Mev would predict damage rates of
negligible importance relative to lower energy damage rates. However, high energy
protons have been shown[1-3] to produce considerable damage in silicon due to nuclear
spallation. The resulting over-all energy dependence as controlled by the above
mechanisms exhibits a low energy cut-off, rising steeply to a peak degradation
rate in the vicinity of a few Mev depending upon the device considered and then
falling off with increasing energy as approximately $E^{-1}$. At about 100 Mev
plateau is reached wherein damage is relatively independent of further increase
in energy because of spallation mechanisms.

In the course of proton radiation effects experiments, many laboratories have obtained and published energy dependence data. In these experiments, however, experimental techniques often vary considerably and the published data exhibit considerable conflict in the exact energy dependence of the degradation rate. Recent experiments[4] have confirmed the nonlinearity of solar cell characteristics under proton bombardment which, because of different experimental techniques, has been responsible for a major portion of the disagreement observed in the energy dependence of proton damage. Specifically, it has been observed that K values, which are derived from minority carrier diffusion length measurements for proton irradiated solar cells, are a strong function of the illumination level utilized in their determination. In order to resolve these disagreements and obtain a meaningful energy dependence characteristic for solar cell power supply design, an experiment was designed to accomplish two objectives: (1) Provide practical energy dependence data on contemporary solar cells with consistent damage parameters over the energy range from 5 to 450 Mev, and (2) Determine the energy dependence of the observed variation in minority carrier diffusion length with injection level in silicon for use in correcting earlier experimental data.

To assist in attaining the objectives outlined above, an experiment was conducted with the 32 Mev proton linear accelerator at the University of Southern California. Energy dependence data were obtained utilizing foil absorbers to vary the energy between 6.7 Mev and 27 Mev. The purpose of this report is to present the results of this experiment and compare these results with previously obtained results at 95.5 Mev and 450 Mev.

II.  DESCRIPTION OF EXPERIMENTS

The primary objectives of this experiment were the acquisition of quantitative experimental data on (1) the energy dependence of proton radiation damage in silicon and gallium arsenide solar cells and (2) the energy dependence of the variation in minority carrier diffusion length with injection level. These experiments were conducted in a manner similar to those described in a previous report[4]. Since a detailed description of the experimental techniques and apparatus is included in this previous report, the descriptions presented below will only summarize the general experimental techniques except in those cases where additional

functions were required. The remainder of this section is devoted to descriptions of the test specimens, measurement performed on the test specimens, dosimetry measurements of beam energy intensity and distribution, and the general experimental techniques followed in the conduct of this experiment.

## Solar Cell Specimens

The test specimens consisted of both silicon and gallium arsenide solar cells and additional silicon material for determination of proton induced energy levels through Hall effect measurements. The silicon solar cells used were Hoffman 1 ohm-cm p on n silicon solar cells (symbol CEG), Western Electric 1 ohm-cm n on p silicon solar cells (symbol HEW), Hoffman 10 ohm-cm n on p silicon solar cells (symbol OCO), and RCA p on n gallium arsenide solar cells (symbol H). This group of solar cells was chosen because of the large amount of data existing on these types of cells, their established quality and reproducibility, and their representation of state-of-the-art devices currently available. The Hall specimens consisted of both p and n-type silicon with resistivities in the range of 1 ohm-cm to 100 ohm-cm. The Hall specimens were pre-cut to the conventional six-arm cross configuration for post-irradiation measurements of Hall effects.

Of the group of solar cells finally selected through initial measurements of I-V characteristics and minority carrier diffusion lengths, several cells of each type were subjected to electron irradiation. The purpose of this prior electron irradiation was to establish for this particular group of cells standard short circuit current degradation slopes and empirical relationships between short circuit current density and minority carrier diffusion lengths for later use in the proton experiment.

## Solar Cell Measurements

The measurements performed on the test solar cells consisted of I-V characteristics, diffusion length measurements utilizing both the Van de Graaff accelerator and the empirical short circuit current relationship, and the variation of minority carrier diffusion length with injection level. Of these measurements, the I-V characteristics and the minority carrier diffusion length measurements using calibrated short circuit current-diffusion length relationships were performed

at the irradiation site, while diffusion length measurements with the Van de Graaff and the determination of minority carrier diffusion length dependence on injection level were performed following the experiment at the STL facilities. Additional I-V characteristics were obtained at the STL facility for comparison with those obtained at the irradiation site to insure adequate calibration and an accurate measure of any annealing that may have occurred between the two sets of measurements.

The I-V characteristics were obtained with a $2800^{\circ}$K unfiltered tungsten illumination source. The illumination intensity was maintained at the same level used in all previous experiments. This illumination intensity is approximately 110 mw/cm$^2$ nominal sunlight equivalent for a conventional solar cell having a minority carrier diffusion length of 100 microns. Short circuit currents were acquired from these I-V characteristics to determine degradation as a function of integrated flux during the course of the experiment. In addition, these short circuit currents were used to obtain a minority carrier diffusion length under one sun equivalent illumination for the determination of practical $\Upsilon$ values utilizing the previously obtained diffusion length versus short circuit current empirical relationships. This technique for obtaining minority carrier diffusion lengths at the irradiation site under one sun illumination conditions is described in detail in Reference 4.

Upon returning to the STL facilities, measurements of minority carrier diffusion lengths with the Van de Graaff accelerator as a function of injection level were initiated. Briefly, this technique consists of using a modulated electron beam from the accelerator to determine the actual minority carrier diffusion length while simultaneously varying the excess carrier concentration through illumination by an exterior variable intensity light source[4]. These diffusion length data were compared with the previously obtained minority carrier diffusion lengths at the irradiation site.

The Hall specimens bombarded in the experiment were further measured and analyzed at the STL facilities using conventional techniques described in a previous report[5]. The purpose of these measurements was to determine the nature and position of some of the energy levels produced by the proton irradiation.

Dosimetry

To obtain as accurate knowledge of the radiation environment as possible, particular attention was given to measurement of proton beam energy, distribution, and intensity. The techniques included range energy experiments and a solid state detector-spectrometer for determination of beam energy. Carbon-11 activation and solar cell ionization detectors for determination of beam distribution, an evacuated Faraday cup and solar cell ionization detector for determination of beam intensity, and Polaroid film for determination of beam position and over-all distribution. Although specific details of these techniques appear in a previous report[4], a brief summary of each function will be given below.

The proton energy of the external beam incident on the test specimens was determined with range energy experiments using varying thicknesses of aluminum foil and a solar cell as an ionization detector. Analysis of the resulting Bragg curve yielded a maximum energy incident on the test specimens, located approximately 6 feet from the exit port, of $26.0 \pm 0.5$ Mev. In addition, a solid state junction detector was placed in the beam and a calibrated pulse height analysis yielded an incident energy of $26.0 \pm 0.1$ Mev. For lower proton energy irradiations aluminum foils were stacked in front of the test specimens to degrade the incident beam energy. Calculations performed on proton straggling indicated that a lower limit of about 5 Mev incident proton energy would be available from the primary 32 Mev beam without appreciable energy straggling. Experiments below this 5 Mev limit, therefore, were not attempted because of the rapidly increasing uncertainty in the data caused by energy straggling at these lower energies.

Proton beam distribution and position were determined with Polaroid film exposures, Carbon-11 activations, and an array of solar cells functioning as ionization detectors. Polaroid film exposures were initially used to determine the center line of the proton beam and the approximate beam diameter as a function of distance from the exit port window. After obtaining a beam diameter of sufficient size at a distance of 6 feet from the exit port, the experimental apparatus was installed and further alignments of the apparatus with the beam were obtained with additional Polaroid film exposures. An experimental plate containing nine electron prebombarded solar cells arranged uniformly over 16 $cm^2$ was placed in the experimental apparatus for further determinations of alignment and beam distribution.

When as accurate alignment as possible was obtained with these techniques, Carbon-11 activations were initiated for final determination of alignment and beam distribution.

The use of 0.066-inch thick polyethylene sheets for Carbon-11 dosimetry and the associated techniques of handling and counting are described in detail in a previous report[4]. The polyethylene was pre-cut to 1 $cm^2$ chips, weighed and graded, and mounted on experimental plates over areas ranging from 16 $cm^2$ to 100 $cm^2$. These chips were mounted on plates identical to test specimen plates resulting in accurate placement of the polyethylene chips in the experimental apparatus for determination of beam characteristics. Following the initial alignment and setup procedures outlined above, a series of three Carbon-11 activations were performed at 26 Mev for final determination of beam alignment and distribution.

The results of the Carbon-11 activations are plotted and analyzed to yield isointensity contours. The first Carbon-11 activation performed at 26 Mev yielded the isointensity contour shown in Figure 1. As is observed in the figure, the experimental apparatus is properly aligned in the vertical plane but is out of alignment by approximately 0.2 cm in the horizontal plane. The apparatus was re-aligned and additional Carbon-11 activations were performed to obtain good statistical results for both absolute and relative proton distribution and intensity. The sample position, i.e., the center 4 $cm^2$ of the proton beam is observed to possess a maximum variation in proton intensity of approximately 12 per cent from the center of the beam to the edge of the specimen area.

After completion of the experiments at 26 Mev, aluminum foils were placed in the experimental apparatus to degrade the beam energy to 20 Mev. The foils, in addition to degrading the beam energy, also aid in flattening out the beam distribution through Coulomb scattering in traversing the absorber foils. Additional Carbon-11 activations were performed at 20 Mev. Typical of the isointensity contours obtained is Figure 2 in which the observed variation in intensity across the specimen area is reduced a few per cent from that observed at 26 Mev. In later experiments at lower proton energies, Carbon-11 activations were performed but little usable data were obtained because of the rapidly decreasing activation cross section for Carbon-11 below 20 Mev and the increasing importance of the

ISOINTENSITY   CONTOURS
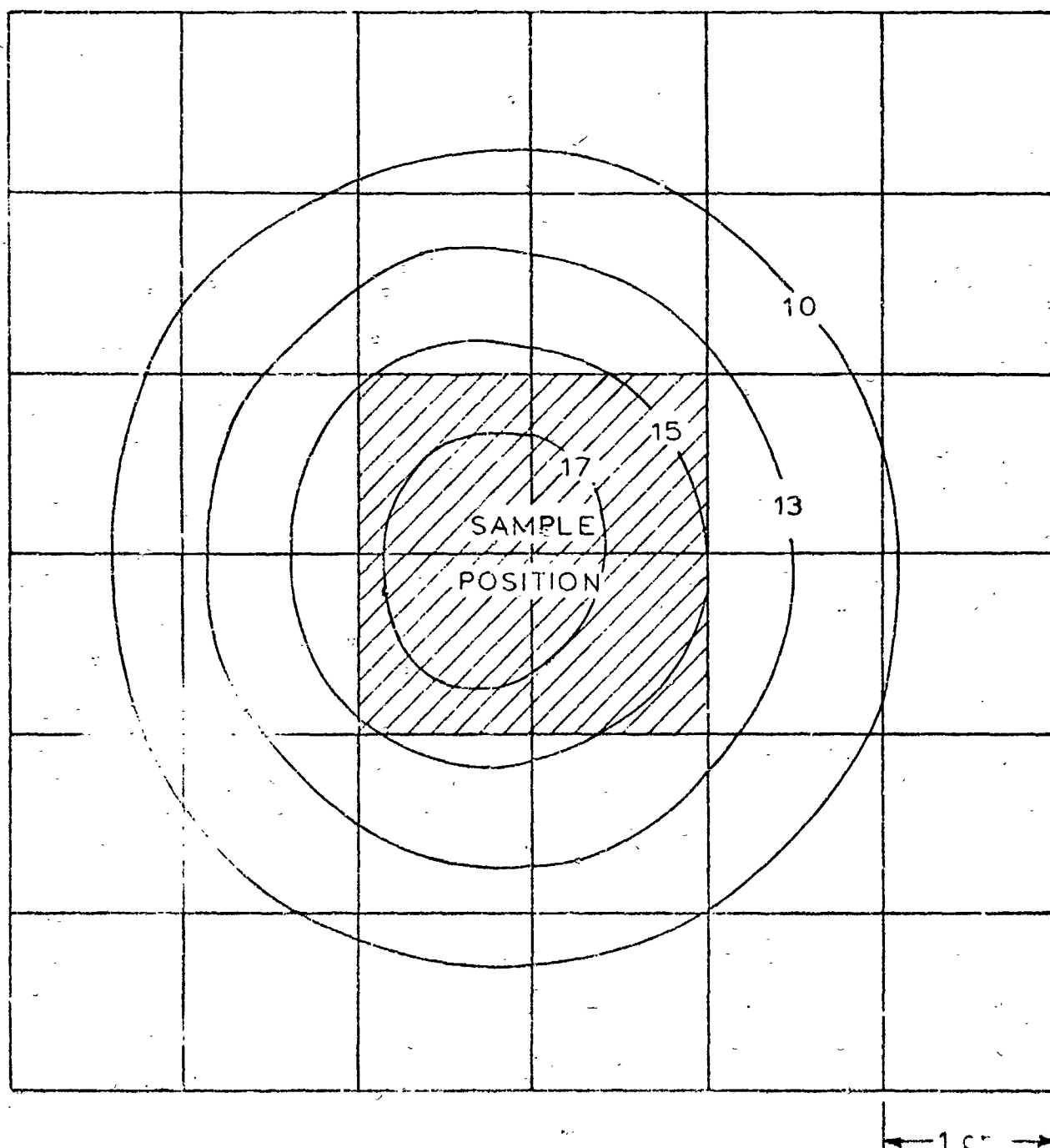for 26 Mev   in units of
$10^8$ p/cm²-sec



Figure 1.   Isointensity Contours Obtained with Carbon-11
Activation at 26.0 Mev

ISOINTENSITY CONTOURS
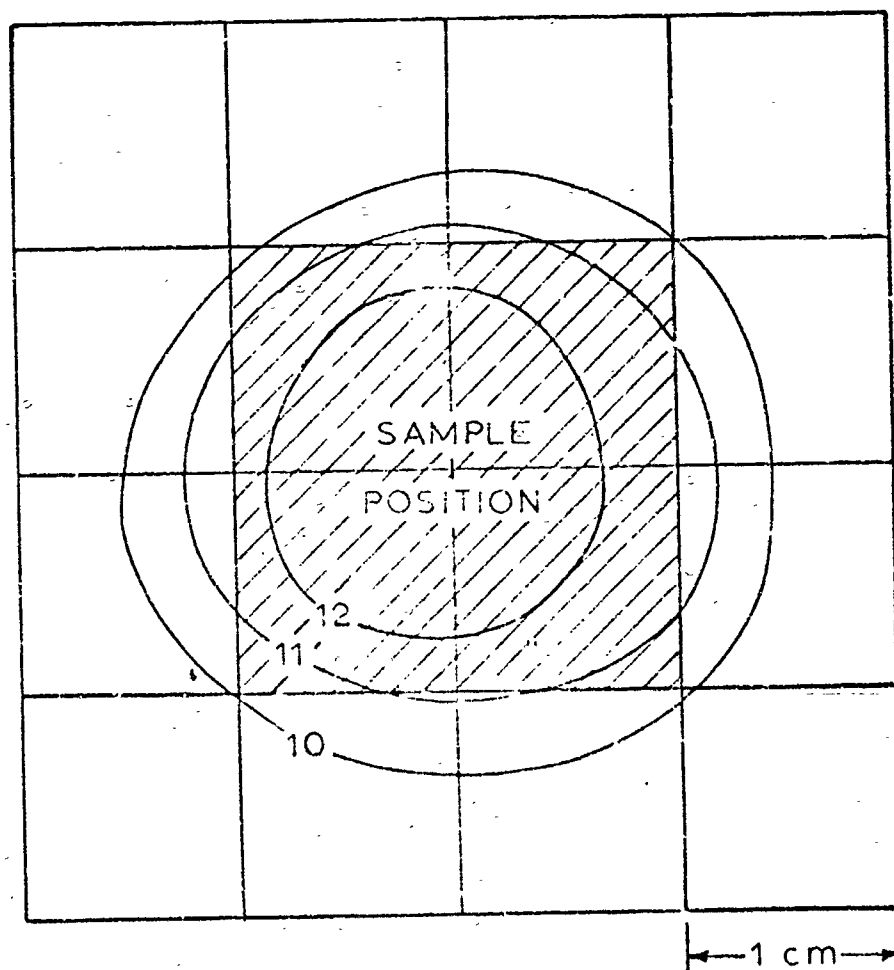for 20 Mev in units of
$10^8$ p/cm$^2$-sec



Figure 2. Isointensity Contours Obtained with Carbon-11
Activation at 20.0 Mev

Nitrogen-13 activation cross section at these energies. The resulting radioactive decay scheme was too complex to be handled by the apparatus on hand at the site. However, the use of successively thicker foils at lower proton energies further reduces the intensity variation across the area through Coulomb scattering. Since the amount of intensity variation across the test specimen is small initially, the decrease in this variation at lower energies can be obtained from extrapolation of data at 26 and 20 Mev with negligible inaccuracy in the over-all intensity determinations.

In addition to using the Carbon-11 activation for determination of relative beam distribution, absolute intensities were obtained from the Carbon-11 activation count rates after including the necessary corrections for counter efficiency, geometry, etc. The proton intensities obtained through Carbon-11 activation were in agreement within 5 per cent with proton intensities obtained with the Faraday cup and solar cell ionization detectors. Since the absolute activation cross section, counter efficiency, and geometric factors are not known with accuracies any better than 5 per cent, it is concluded that the intensities obtained with the Carbon-11 activation technique are in agreement with those obtained by other techniques within the over-all experimental accuracies involved.

Actual proton intensities were obtained in the course of the experiments with an evacuated Faraday cup of conventional design. The evacuated cup included an inner sensing chamber, a back-scatter shield, and a secondary repelling grid. The output of the Faraday cup was coupled to a current integrator which allowed continuous recording of both the proton intensity and the total integrated exposure. The Faraday cup contained an entrance aperture of 10 cm$^2$. The fraction of the total collected charge in the cup attributed to that portion of the beam passing through the sample area was obtained through analysis of the previously described Carbon-11 activations. Initial checkout of the Faraday cup consisted of varying the grid potential from +400 to -400 volts. Negligible change in indicated beam current was observed indicating that forward scattering off the vacuum window and back scattering out of the inner cup had been satisfactorily held to a minimum through cup design. In addition, no ionization breakdown was observed at the high voltages indicating that chamber vacuum was sufficient. The Faraday cup was located in the experimental apparatus immediately behind the test

specimens. At each energy a dummy plate of test specimens was utilized to obtain
the correction factor necessary for the change in intensity incident on the
Faraday cup produced by the test specimen plate. This correction factor was
found to be negligible in all except the lowest energy series of experiments.

In addition to measuring the proton intensity with Carbon-11 activation
and a Faraday cup, a group of electron prebombarded solar cells was placed in
the beam and the resulting ionization currents measured. Knowing the minority
carrier diffusion length in the solar cell and the electron-hole pair generation
rate from handbook values of $dE/dx$, the absolute proton intensity incident on
the solar cell can be determined. The proton intensities obtained with this
technique agreed within 5 per cent with the intensities determined with the
Carbon-11 activation and within 2 per cent with intensities determined with the
Faraday cup.

## Experimental Setup

The experimental fixture utilized in this series of experiments is the
same fixture utilized in previous experiments at Montreal and San Diego with only
slight modifications in the Faraday cup to improve effectiveness for protons of
these energies. The experimental fixture consists of a base on which is mounted
an adjustable platform with adjustment in the vertical and horizontal directions
for fine alignment of instrumentation and test specimens relative to the center
line of the irradiating beam. On this adjustable platform the Faraday cup is
mounted. Immediately in front of the Faraday cup are located a series of rails
for the insertion of experimental plates, Carbon-11 plates, and film. These
rails are also attached to the platform in order that the relative position of
the test speci...s and the Faraday cup be fixed. A remotely operated solenoid
is included on the rails so that test plates may be removed from the beam at
any time during the course of an experiment.

The experimental jig was placed 6 feet from the proton beam exit port
window to obtain maximum beam defocusing with a minimum energy loss in traversing
the air. The foils for further attenuation of the proton beam were placed on
the first rail immediately in front of the test specimens which were located

on adjacent rails. In order to obtain as accurate data as possible, stacking of
test specimens was not performed in this experiment.

## III. RESULTS

Six separate series of experiments were conducted at the five different
proton energies of 26 Mev, 20 Mev, 15 Mev, 10 Mev, and 6.7 Mev. Two experiments
were conducted at 26 Mev because of the importance of this energy and the fact
that experimental errors were most likely to be encountered at this energy due
to the tightness of the beam distribution. The results of these experiments and
the subsequent post-irradiation measurements of the diffusion length dependence
on injection level are presented in this section.

Short circuit current data were obtained from the I-V characteristics and
plotted as a function of integrated proton flux during the course of the irradia-
tion experiments. The resulting degradation curves are shown in Figures 3 through
8. The slope of the degradation characteristic for each of the three types of
cells tested was obtained in the preliminary electron bombardment calibration
experiments as described earlier. These slopes, found to be 6-1/4 ma/cm$^2$ per
decade for the 1 ohm-cm p on n and n on p cells and 7-1/4 ma/cm$^2$ per decade for
the 10 ohm-cm n on p cells, are indicated in each of the figures. The slightly
higher than normal slope obtained for the 10 ohm-cm n on p solar cells is thought
to be attributed to back surface effects causing either minority carrier reflec-
tion or optical reflection off the back surface of the cell to be a significant
contribution to the observed short circuit currents. As is observed in the
figures, the resulting data points fit the linear slopes quite accurately. The
$I_{sc}$ values to be used in determining the energy dependence were obtained at the
intersection of the standard slope applied to each individual solar cell with
19 ma/cm$^2$. Gallium arsenide solar cells were irradiated at 10 Mev and 26 Mev
as shown in Figures 4 and 8, respectively. In these figures the short circuit
currents shown are total currents for the 1 cm x 2 cm devices for convenience
in comparison with silicon cells on the same scale. As shown by the data, the
gallium arsenide cells are significantly more radiation resistant than silicon
cells, and complete degradation characteristics were not attainable within the
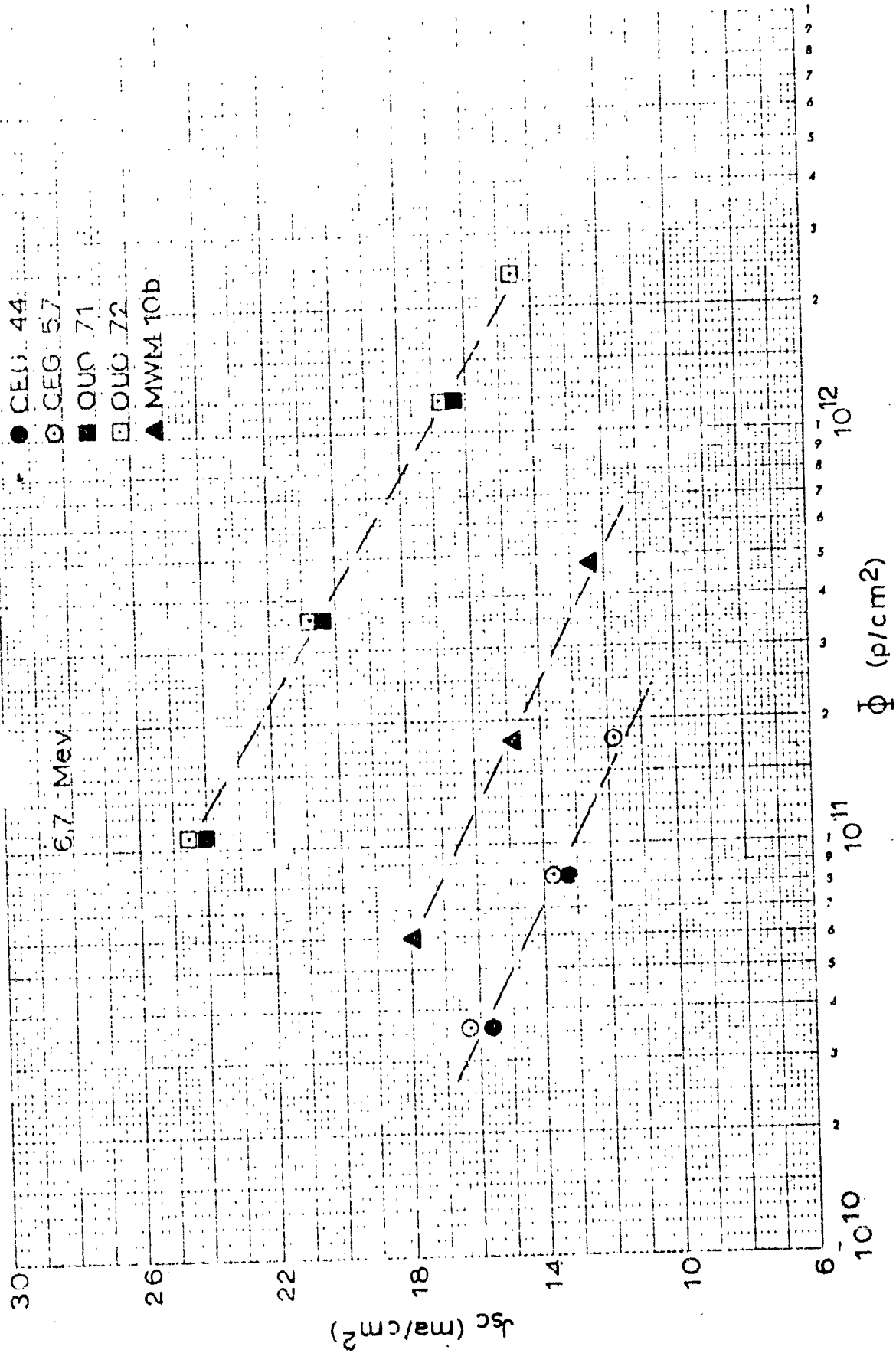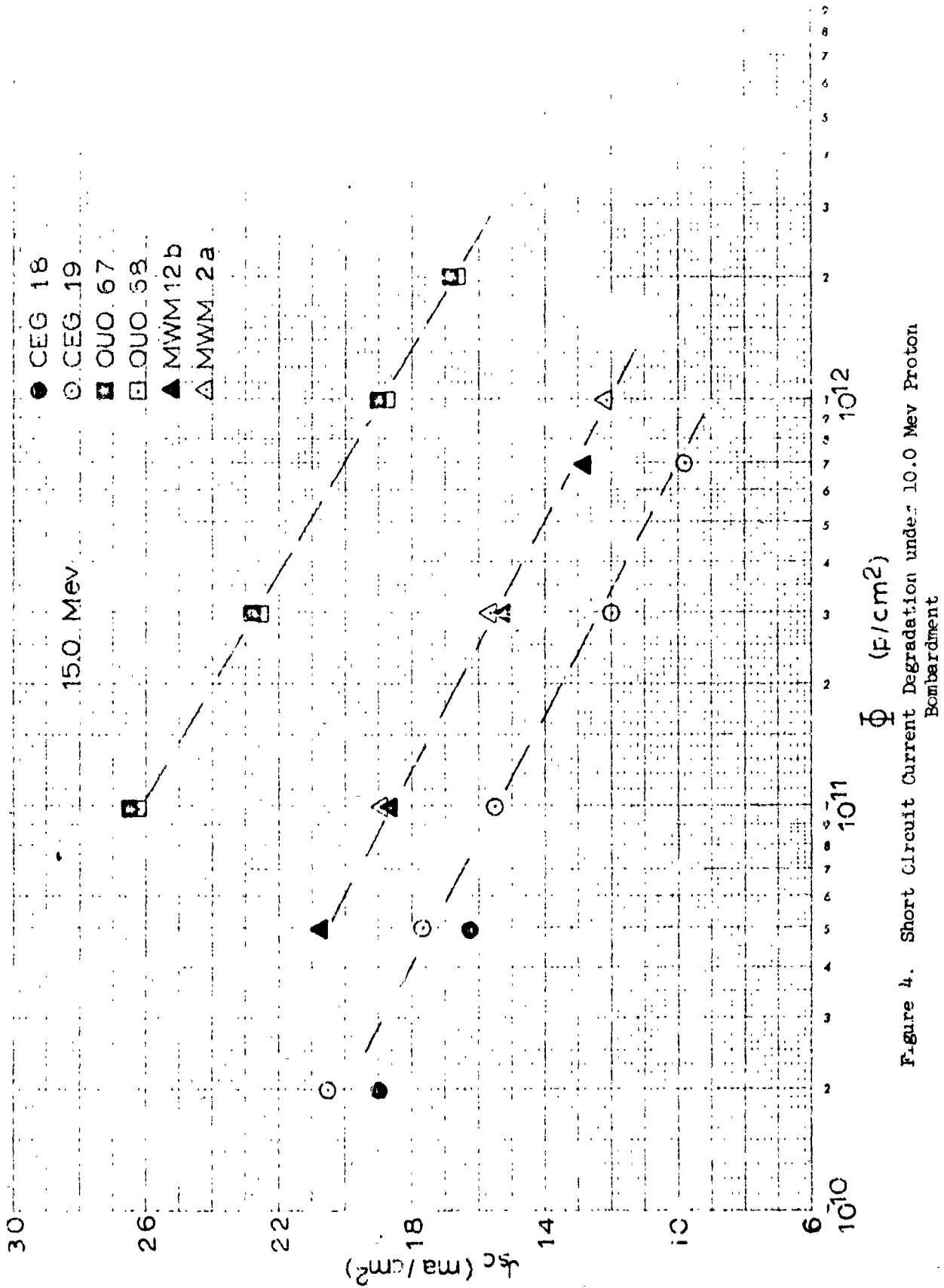beam time available.

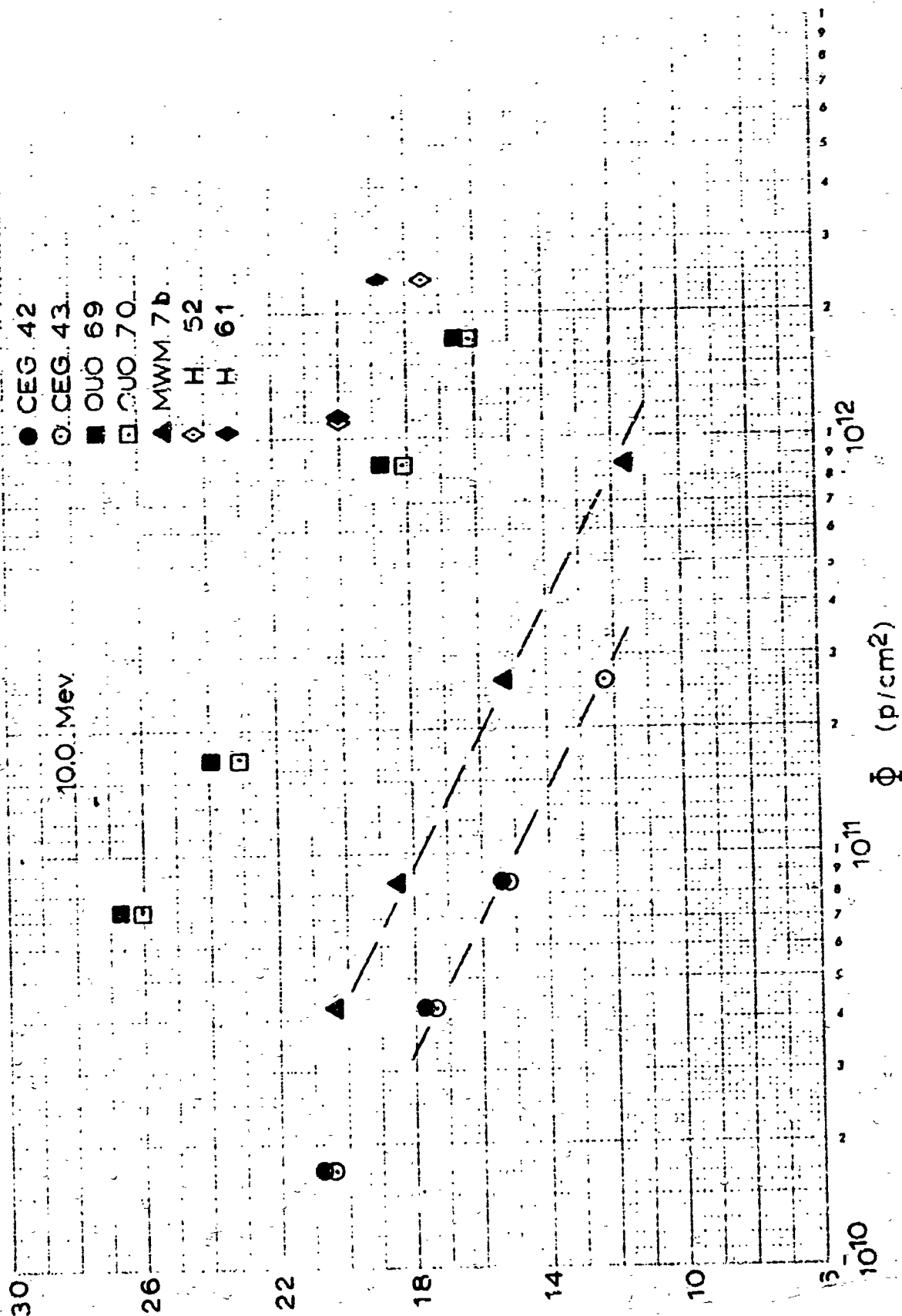Figure 3. Short Circuit Current Degradation under 6.7 Mev Proton Bombardment

Figure 4.  Short Circuit Current Degradation under 10.0 Mev Proton
Bombardment

Figure 5. Short Circuit Current Degradation under 15.0 Mev Proton Bombardment
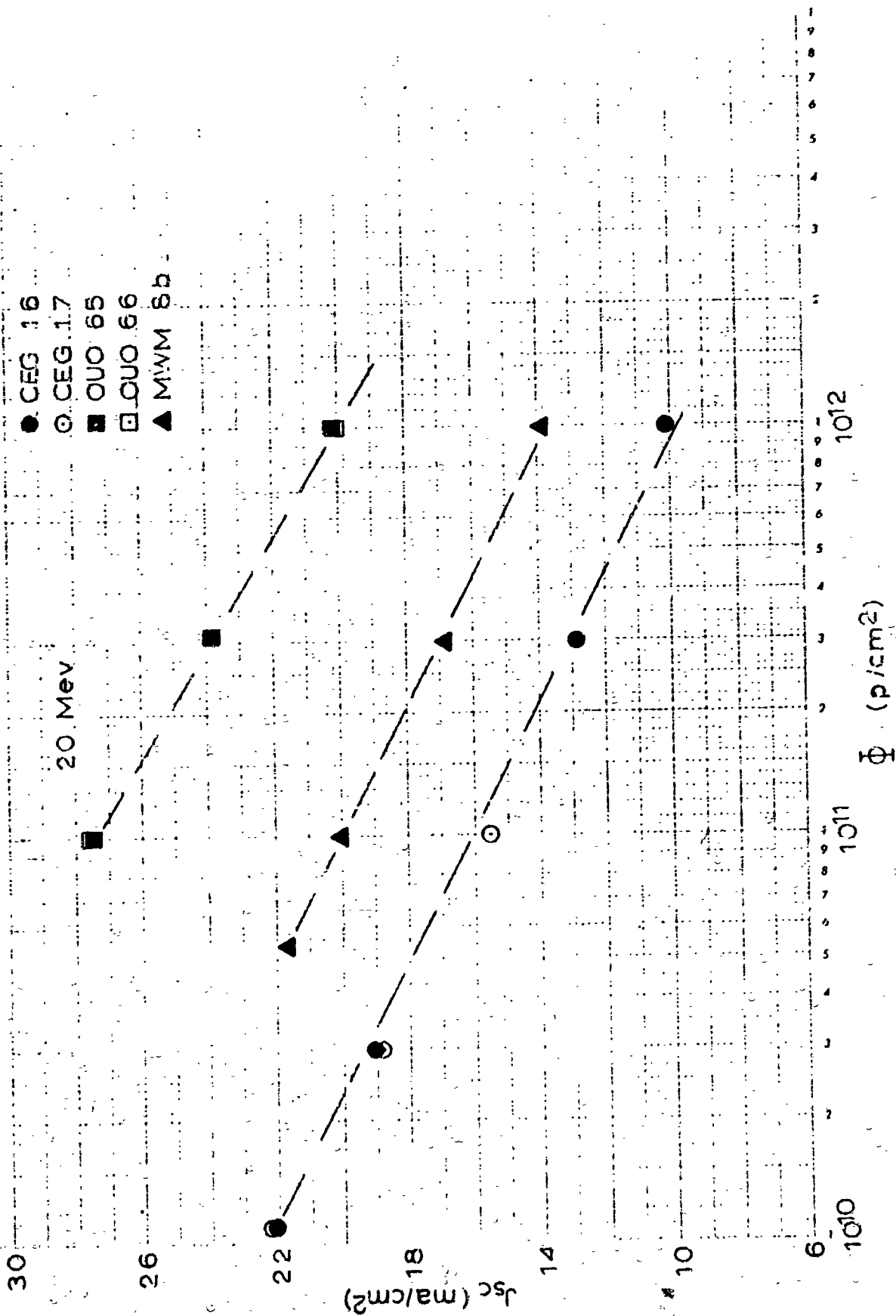
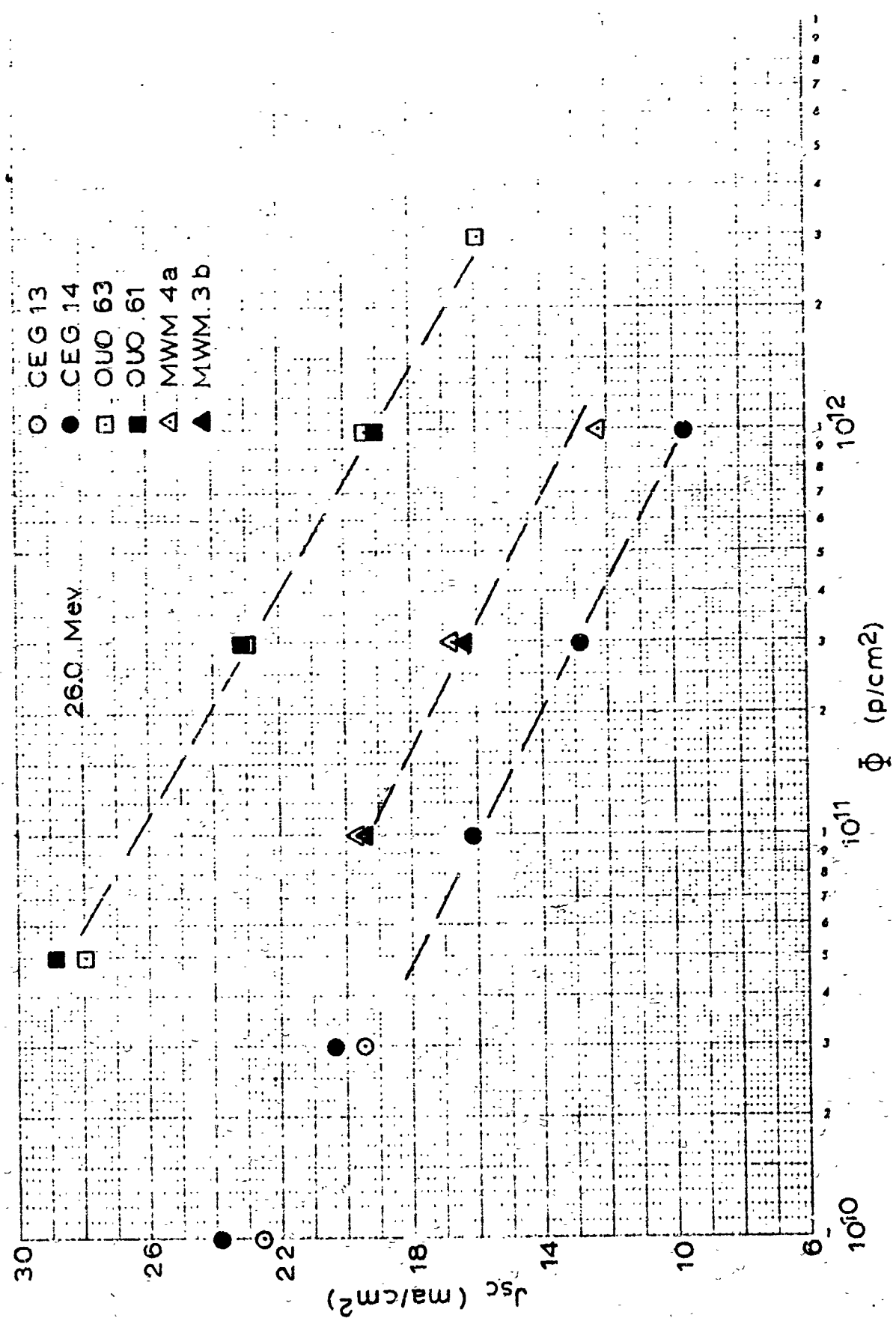Figure 6. Short Circuit Current Degradation under 20.0 Mev Proton Bombardment

Figure 7.   Short Circuit Current Degradation under 26.0 Mev Proton
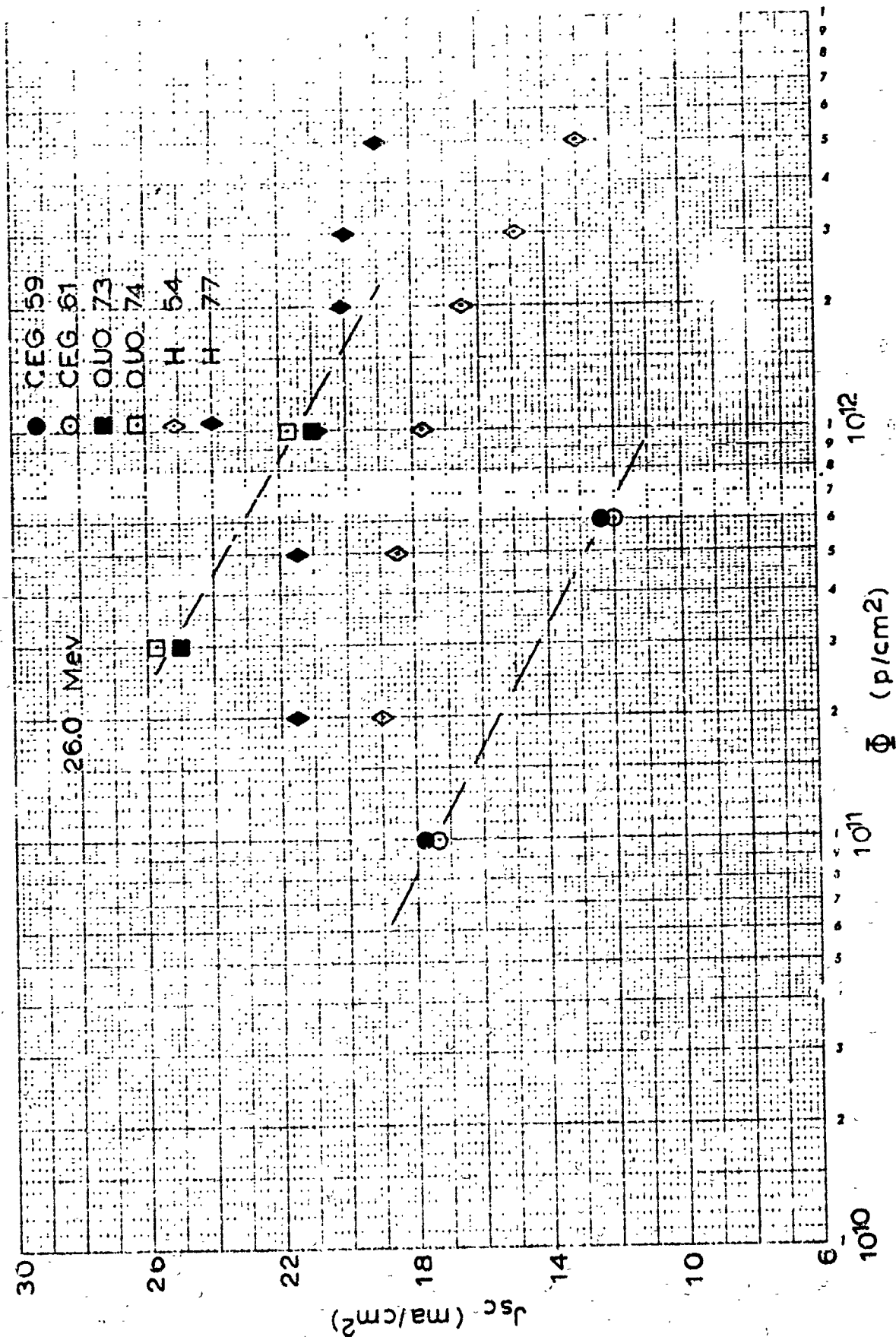Bombardment

Figure 8. Short Circuit Current Degradation for Second Series of Experiments under 26.0 Mev Proton Bombardment

The energy dependence of proton radiation damage in silicon solar cells was obtained using both K* values and reciprocal $\phi_c$ values. A plot of K values for silicon solar cells versus incident proton energy is shown in Figure 9. Included on this plot are data previously obtained at 95.5 Mev and 450 Mev. The 1 ohm-cm n on p Western Electric cells and the 1 ohm-cm p on n Hoffman cells used in this series of experiments are identical to those used at 95.5 Mev rendering direct comparison possible. The K value obtained on older 1 ohm-cm p on n deep diffused silicon solar cells obtained at 450 Mev is shown for comparison with data obtained on a similar type of cell at 95.5 Mev. Two of the series of experiments conducted at USC, i.e., the 6.7 Mev experiments and the 26 Mev experiments, require further comment. At 6.7 Mev, the 0.005-inch thick aluminum vacuum window on the Faraday cup becomes significant in terms of the straggling distribution obtained from the initial 32 Mev beam. To determine beam attenuation produced by this window, a solar cell used as an ionization detector was monitored both with and without a .005-inch aluminum foil in front of it. The correction factor obtained for the Faraday cup was 20 per cent. This correction factor was used in correcting both the 6.7 Mev short circuit current data shown in Figure 3 and the subsequent 6.7 Mev K values shown in Figure 9. At 26 Mev the tightness of the beam distribution rendered alignment during the course of the experiments critical. At the conclusion of the series of experiments from 26 Mev to 6.7 Mev, observation of the raw data indicated that the 26 Mev data did not appear consistent with the remaining data. A second series of experiments were then run at 26 Mev and the results of both 26 Mev experiments are shown in Figure 9.

* K values are derived from the expressions

$$\frac{1}{L^2} = \frac{1}{L_o^2} + K \phi \tag{1}$$

and

$$\frac{d\,(1/L^2)}{d\phi} = K \tag{2}$$

where K is a measure of the radiation sensitivity of the bulk silicon minority carrier diffusion length. The principal advantage of K values is their independence of solar cell surface characteristics, illumination source spectrum, and optical reflectivity effects. For any particular type of solar cell, an empirical relationship can be established between K values and $\phi_c$ values. This relationship, however, is dependent upon the spectral content of the illuminating source used for obtaining the $\phi_c$ values.
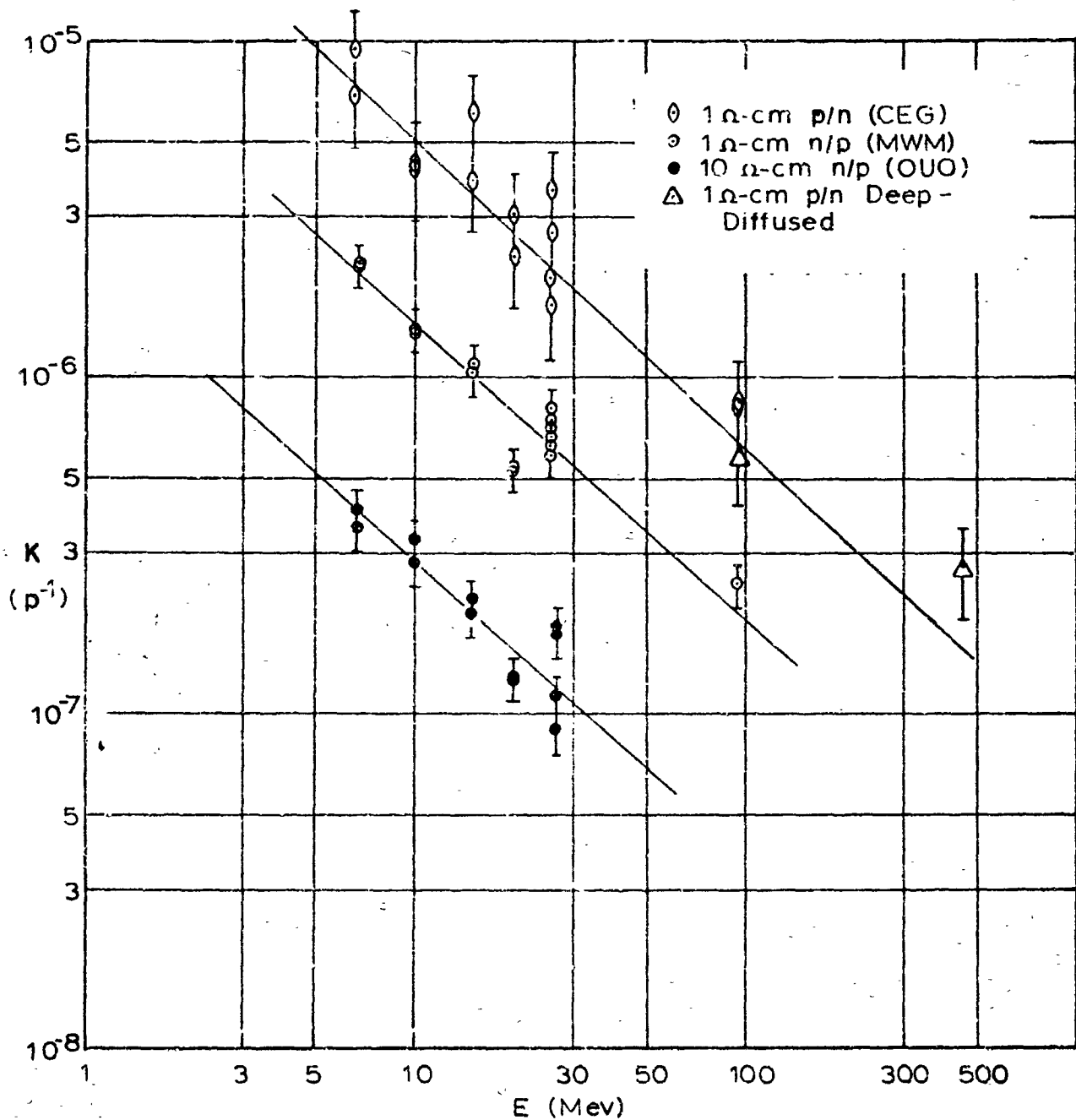
Figure 9.  Proton Energy Dependence of Silicon Solar Cells
Determined by K Values under One Sun Illumination

As described in a previous section, the accuracies to which proton beam energy and integrated proton flux were determined are better than $\pm$ 5 per cent. Therefore, the major uncertainty in the experimental data points is the variation between solar cells in any given group. These variations in response of solar cells to radiation are approximately 15 per cent for n on p cells and approximately 30 per cent for p on n cells in lots of the size used in this experiment. For these reasons, uncertainty limits of the above described amounts are placed on each data point. A straight line having a slope proportional to $E^{-1}\ln(Em/2Ed)$, which is approximately equal to $E^{-0.93}$, is drawn through each group of data points. This straight line shows good agreement with all the experimental data points in the range from 6.7 Mev to 95.5 Mev. The data point on older deep diffused 1 ohm-cm p on n silicon solar cells at 95.5 Mev is in good agreement with the slope shown for contemporary 1 ohm-cm p on n solar cells, whereas the data points for 25 similar cells tested at 450 Mev lie significantly above this slope. This behavior supports the departure from simple theory of high energy proton irradiation damage on solar cells predicted on the basis of theoretical calculations described in previous reports[2,3].

Since it has been previously shown[4] (and will again be demonstrated in a later section) that diffusion length measurements on proton bombarded cells vary with injection level, it is important to remember that the K values shown in Figure 9, as well as in all previous work, are K values obtained at approximately one sun illumination levels. For diffusion length measurements obtained at lower injection levels, i.e., by either electron or proton beams, measured K values will differ considerably from those shown in Figure 9 because of the lower injection levels produced by these techniques. The data on K values shown in Figure 9 were obtained from diffusion length measurements acquired under one sun intensity as described in the previous section.

A similar energy dependence is obtained using reciprocal $\phi_{Lc}$ values as shown in Figure 10. The energy dependence based on reciprocal $\phi_{Lc}$ values is observed to be identical to that based on K values with only slight relative shifts between different groups of cells depending on unrelated but varying characteristic differences between groups of cells such as surface characteristics and back surface reflectivities and/or recombination velocities. As in the previously
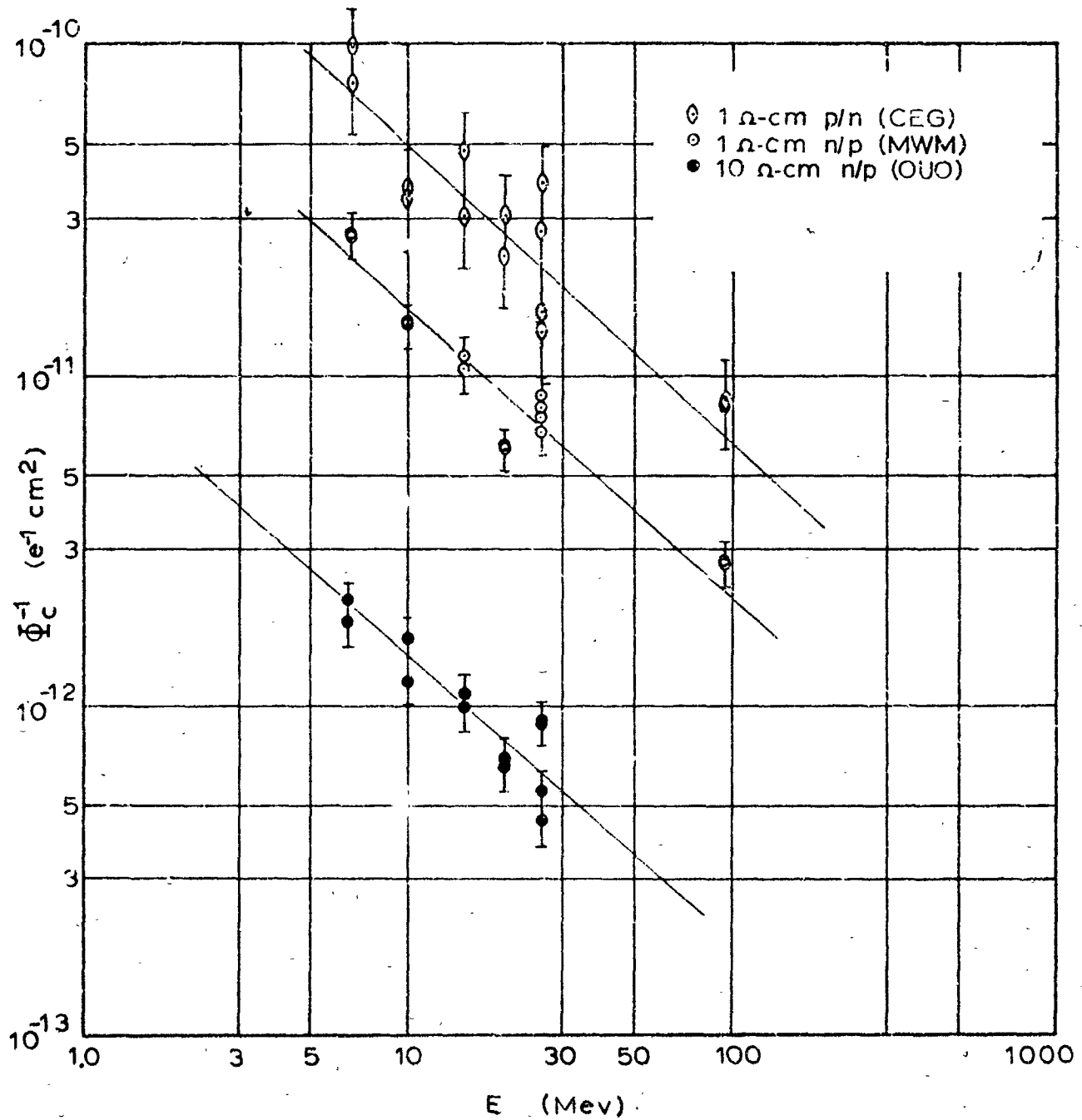
Figure 10    Proton Energy Dependence of Silicon Solar Cells
Determined by Reciprocal Critical Flux Values

discussed Figure 9, the data shown in Figure 10 support the theoretical predictions of an energy dependence linearly proportional to $E^{-1}\ln(Tm/2Ed)$.

In summary, all experimental data obtained in the energy region from 6.7 Mev to 450 Mev support a linear inverse energy dependence of proton damage in silicon for energies up to about 100 Mev. Above 100 Mev gradual departure from the inverse energy dependence is observed at 450 Mev as predicted on the basis of theoretical relationships involving spallation mechanisms.

Following the series of experiments at the USC proton accelerator site, the test specimens were returned to STL and an extensive series of post-irradiation measurements were performed on the effect of injection level on observed minority carrier diffusion lengths. The dependence of observed minority carrier diffusion length over the range of injection levels of practical importance had earlier been observed and measured[4]. The techniques utilized in measuring the injection level dependence on this group of cells were identical to the techniques previously used[4]. Representative cells from each irradiation energy group were tested. The results of these measurements are shown in Figures 11 through 15 as a function of bombarding proton energy. Several interesting trends are observed in the data. The characteristic shape of the curves relating minority carrier diffusion lengths to injection levels is essentially independent of the proton energy used to produce the radiation damage. Also, both the p on n 1 ohm-cm solar cells and the n on p 10 ohm-cm solar cells have a steeper dependence of apparent minority carrier diffusion length on injection level than the n on p 1 ohm-cm solar cells. In addition, none of the curves show any evidence of approaching an upper limit of diffusion length at the higher injection levels.

The original minority carrier diffusion lengths of this group of solar cells ranged from 150 to 225 microns. After the series of proton irradiations at USC were completed, the irradiated solar cells had minority carrier diffusion lengths ranging from 5 microns to 50 microns. The solar cells used for the post-irradiation measurements of minority carrier diffusion length versus injection level, were chosen for as wide a range of radiation damage as possible. In order to study the effect of proton energy on the injection level dependence for each particular type of solar cell, the data were normalized to zero injection level minority
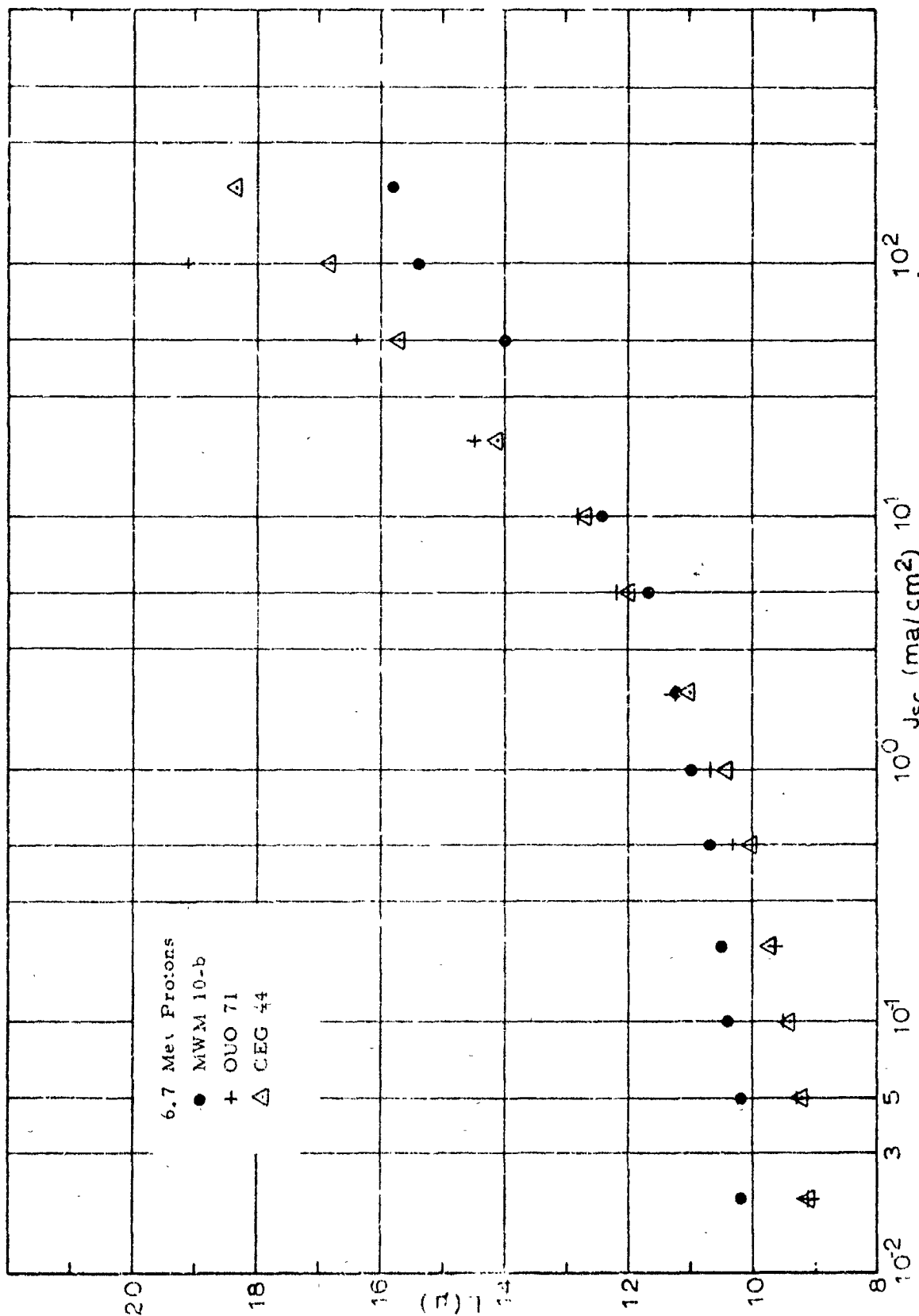
Figure 11. Injection Level Dependence of Minority Carrier Diffusion
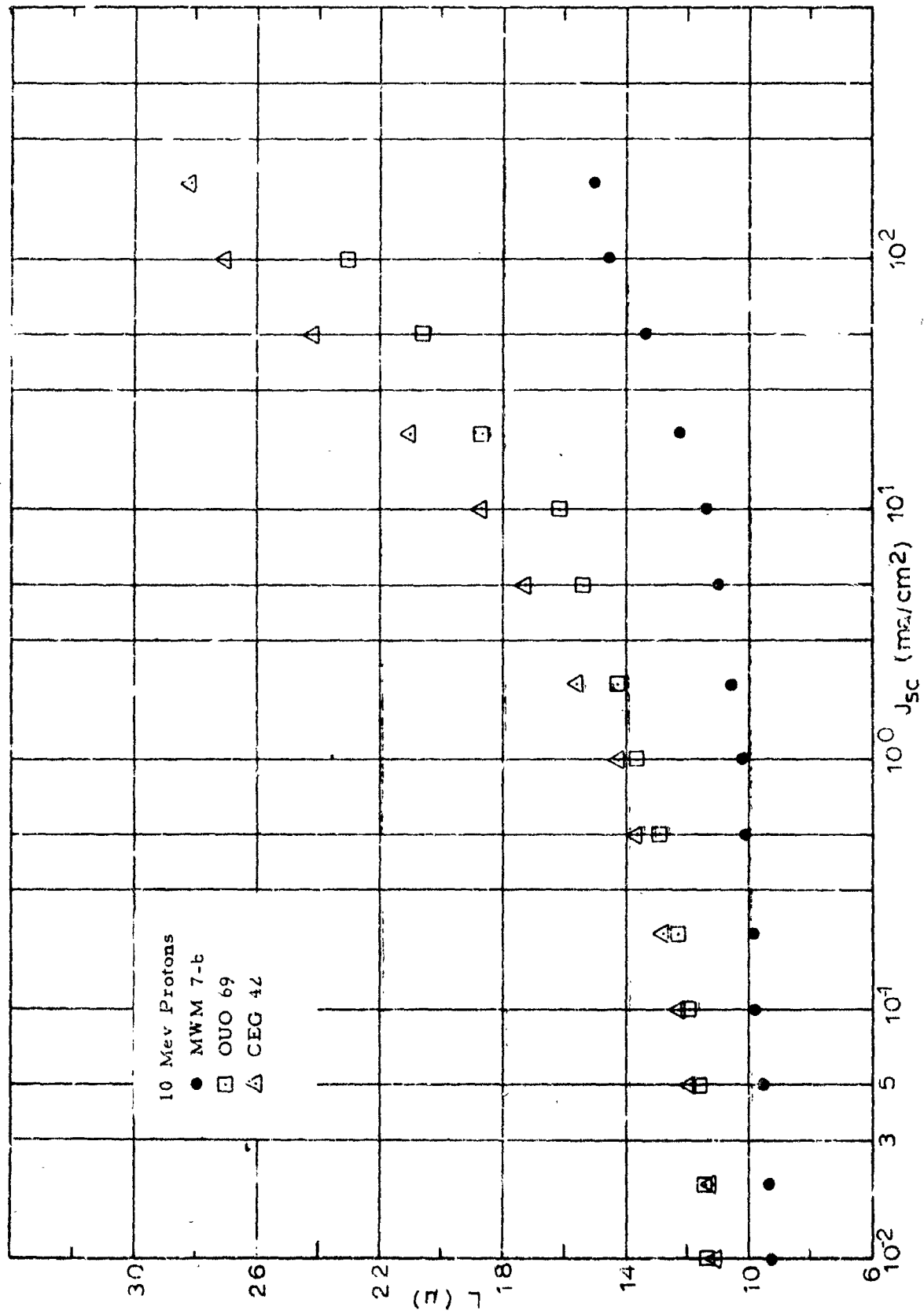Length for Silicon Solar Cells Irradiated with 6 7 Mev Protons

Figure 12.  Injection Level Dependence of Minority Carrier Diffusion Length for Silicon Solar Cells Irradiated with 10.0 Mev Protons
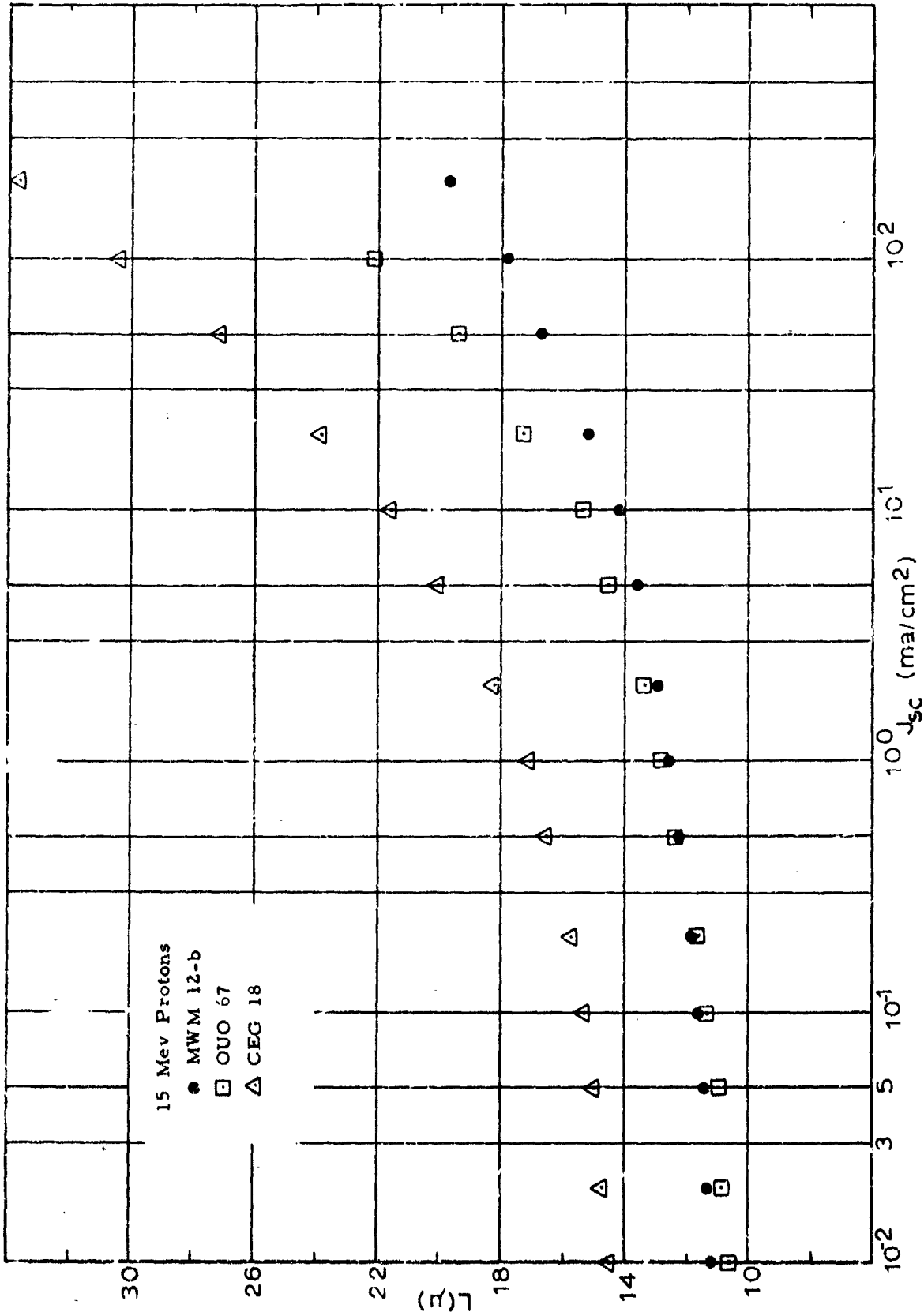
Figure 13.  Injection Level Dependence of Minority Carrier Diffusion Length for Silicon Solar Cells Irradiated with 15.0 Mev Protons
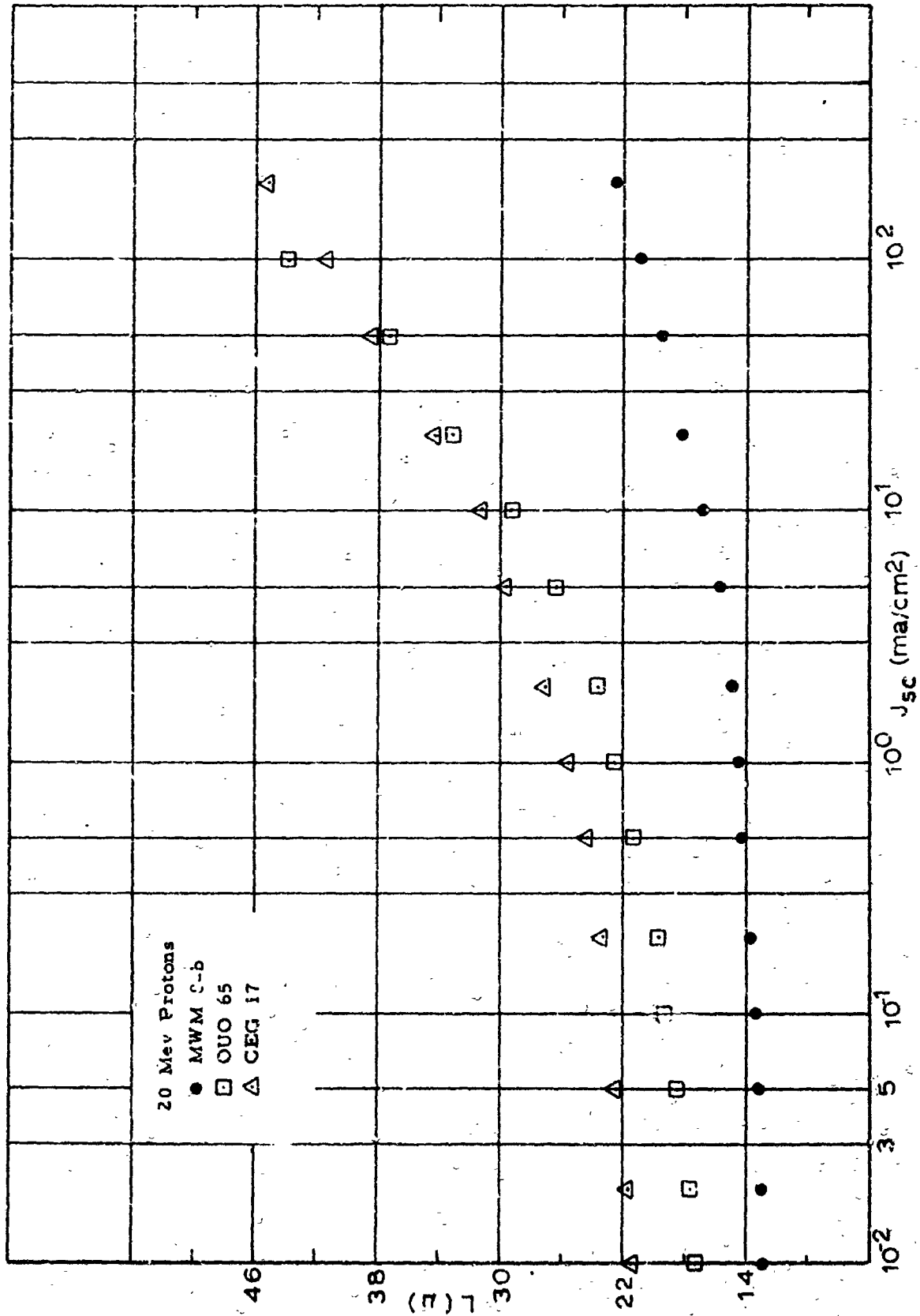
Figure 14. Injection Level Dependence of Minority Carrier Diffusion Length for Silicon Solar Cells Irradiated with 20.0 Mev Protons
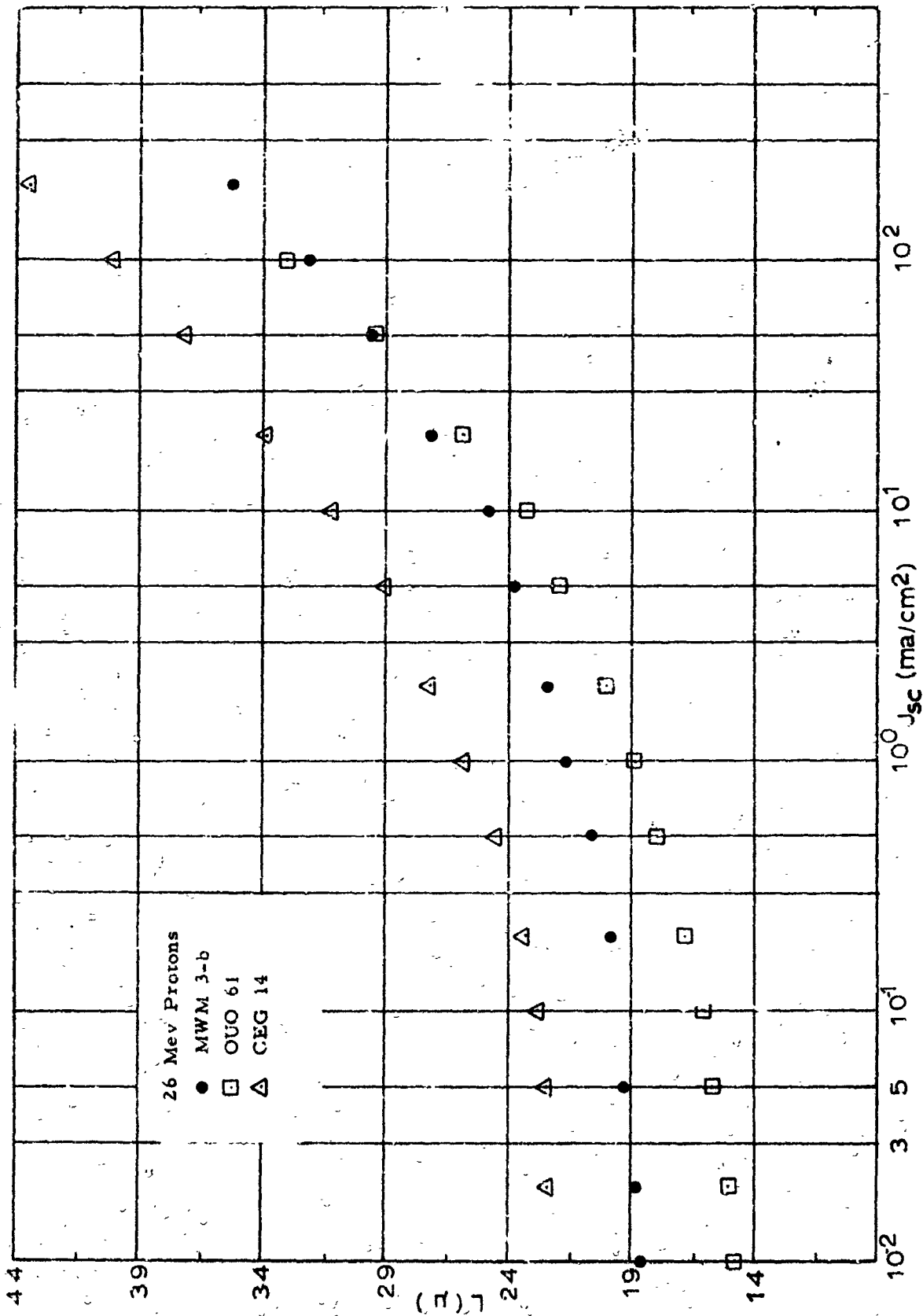
Figure 15. Injection Level Dependence of Minority Carrier Diffusion Length for Silicon Solar Cells Irradiated with 26.0 Mev Protons

carrier diffusion lengths and replotted as an energy dependent family of curves for each type of cell as shown in Figures 16 through 18. Several tentative conclusions can be drawn from the results shown in Figures 16 through 18. First, the increase in apparent diffusion length with increasing injection levels is a fractional increase of the zero injection level diffusion length regardless of the absolute magnitude of the zero injection level diffusion length. Secondly, the proton energy dependence of the apparent diffusion length variation with injection level is either slight or nonexistent in the proton energy range from 6.7 Mev to 95.5 Mev. Finally, the magnitude of this effect is sufficient to require care in the planning of proton radiation damage experiments on silicon devices at any proton energy.

There are two general shortcomings to the injection level dependence data presented in Figures 11 through 18. First of all, the technique for obtaining these data results in a nonlinear excess carrier concentration as a function of depth in the solar cell. Hence, the application of these data to Hall, Shockley-Reed analysis in an effort to obtain information concerning energy level structure is extremely difficult. Secondly, the resolving power of this technique appears to be inadequate to delineate the nature of a second order energy dependence term for the effect. However, the primary purpose of these measurements was to determine the existence of an injection level dependence of importance over this energy range, and that objective has been conclusively attained by the data presented in Figures 11 through 18.

## IV.  SUMMARY AND CONCLUSIONS

A series of proton irradiation experiments were performed with the University of Southern California 32 Mev proton linac covering the energy range from 6.7 Mev to 26 Mev. The results of these experiments are incorporated with the results of previous experiments at 95.5 Mev and 450 Mev on similar types of test specimens in an effort to determine the energy dependence of proton radiation damage in silicon. The results of this work support the proton energy dependence predicted on the basis of theoretical relationships involving simple displacement theory, Coulomb scattering, and spallation mechanisms. The resulting energy dependence is found to be approximately inversely proportional to proton energy
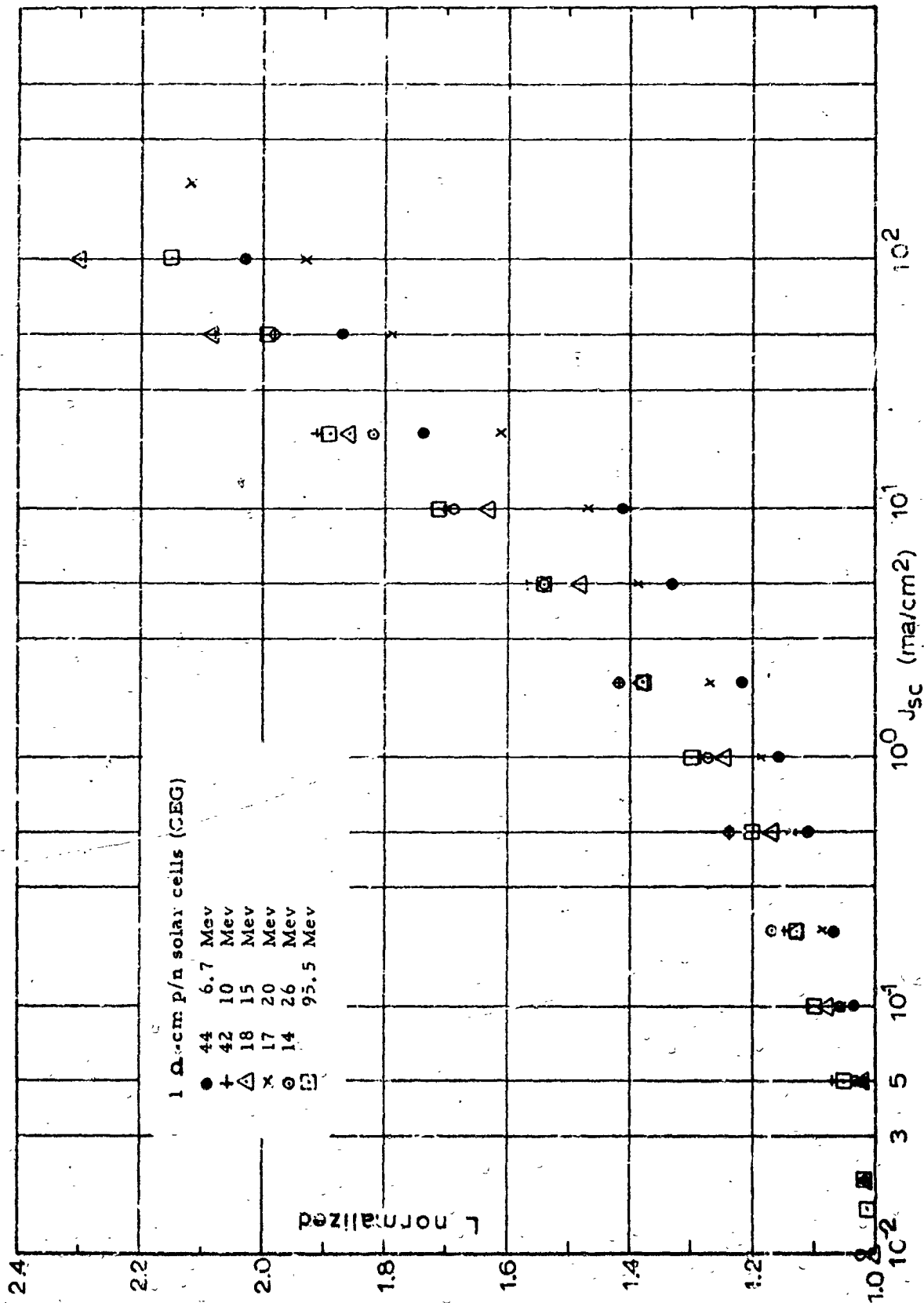
Figure 16. Minority Carrier Diffusion Length Injection Level Dependence of
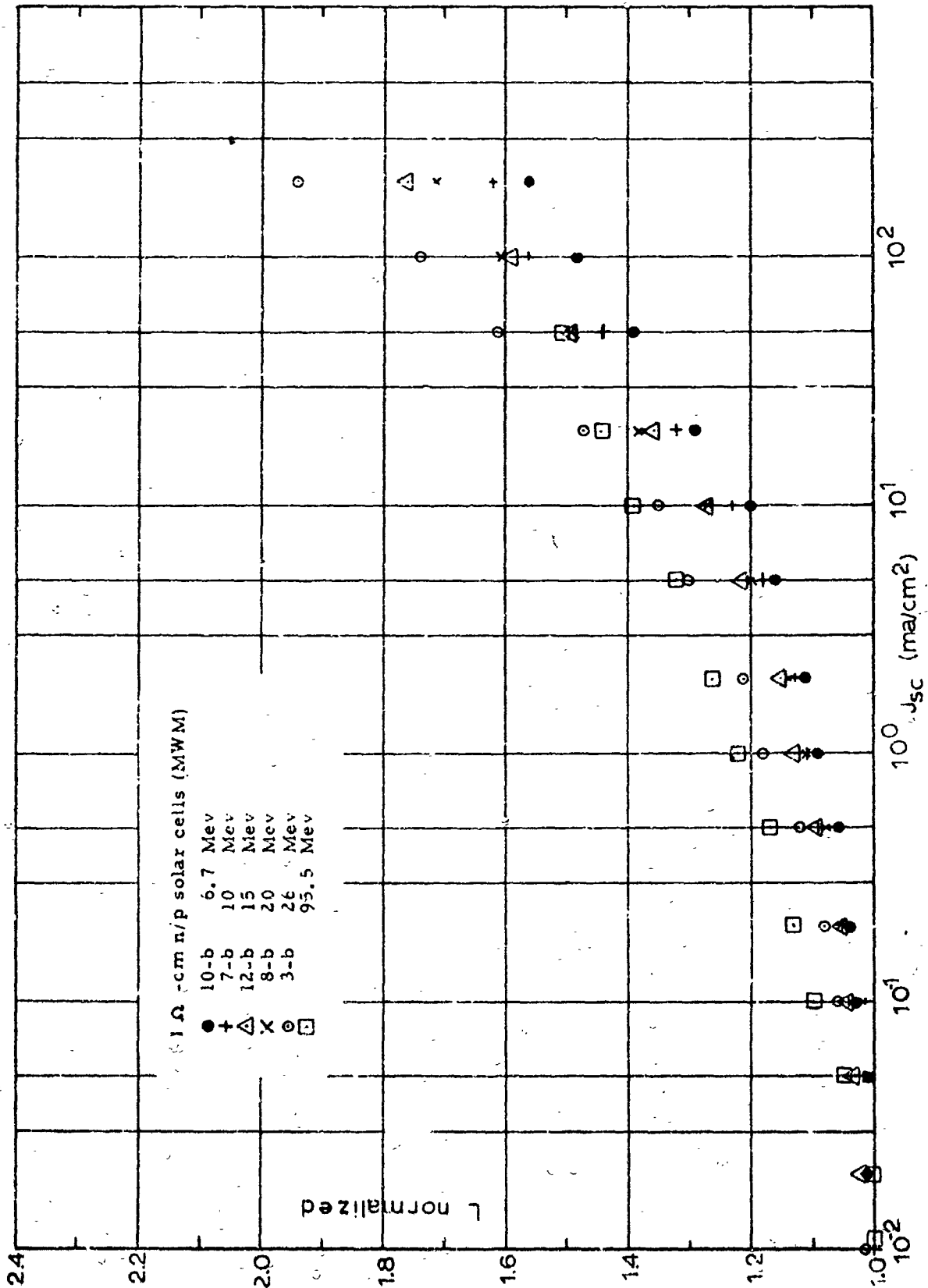Hoffman 1 ohm-cm p on n Silicon Solar Cells as a Function of
Proton Energy

Figure 17. Minority Carrier Diffusion Length Injection Level Dependence of
Western Electric 1 ohm-cm n on p Silicon Solar Cells as a Function
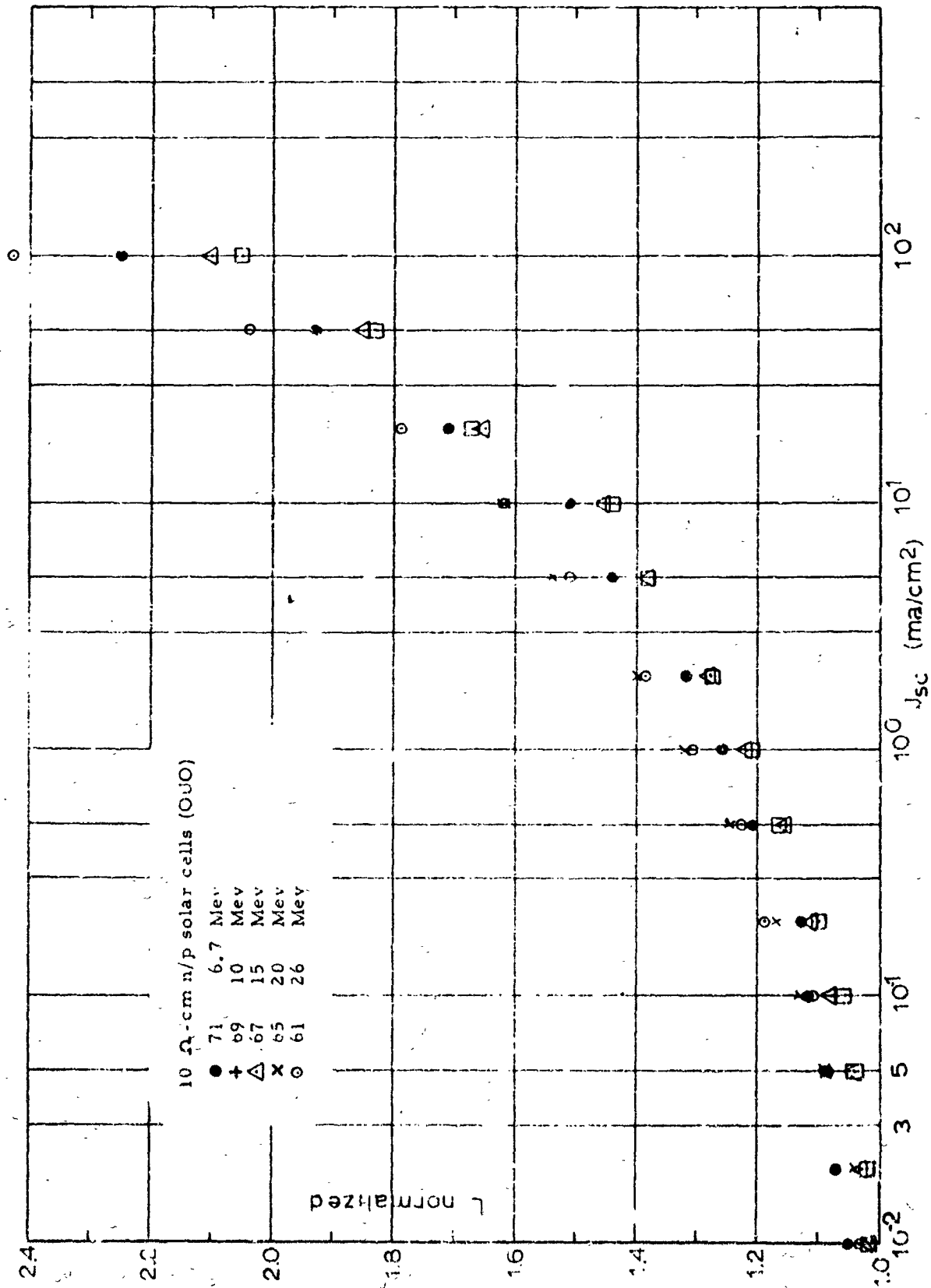of Proton Energy

Figure 18. Minority Carrier Diffusion Length Injection Level Dependence of Hoffman 10 ohm-cm n on p Silicon Solar Cells as a Function of Proton Energy

for energies up to about 100 Mev.  At energies above 100 Mev, the damage dependence
on further increases in proton energy is found to become gradually less, theoreti-
cally approaching a plateau independent of proton energy because of the important
contributions from spallation induced defects.

Additional experimental evidence of the dependence of minority carrier
diffusion length and hence, K values, on the injection level used to determine
these energy dependences has been presented.  At least to first order terms in
energy, there is no energy dependence of the apparent diffusion length dependence
on minority carrier injection level.  It has also been shown that the changes in
observed minority carrier diffusion lengths as a function of injection level
can be expressed in the initial stages as fractional changes of the zero injection
level diffusion length independent of the amount of radiation damage existing in
the silicon base material.  Though the application of Hall, Shockley-Reed statis-
tics predicts an injection level dependence of recombination center controlled
minority carrier diffusion lengths    silicon, the injection level range over
which this dependence actually occur appears to be important in solar cell
experiments involving proton irradiations but     electron irradiations.

The experimental techniques utilized in these studies to obtain injection
level dependence are designed primarily to obtain measurements of the magnitude
of the effect as applied to silicon solar cells.  For determination of the actual
energy level structures involved under electron and proton irradiations, these
measurements would have to be performed in a somewhat different manner to yield
experimental data conveniently applicable to analysis through the use of Hall,
Shockley-Reed recombination statistics.

In conclusion, these experiments have shown that the energy dependence
of proton radiation damage in silicon is in agreement with theoretical relation-
ships.  However, the absolute magnitude of the damage rate characteristic as a
function of energy depends upon the injection level at which the energy dependence
is determined.  In this report the energy dependence has been shown at injection
levels approximately equivalent to one sun illumination for silicon solar cells
in order that the data be of direct practical value in the design of solar cell
power supply systems.  The utilization of these data for other proton radiation

damage problems in silicon will require an evaluation of the injection levels to be experienced under normal operation followed by a corresponding shift of the magnitude of the damage constant to account for the change in apparent damage as a function of injection level.

# REFERENCES

1. J. M. Denney, R. G. Downing, "Final Report on Charged Particle Radiation Damage in Semiconductors, I: Experimental Proton Irradiation of Solar Cells," Contract NAS5-613, 8987-0001-RU-000, 15 September 1961.

2. J. M. Denney, R. G. Downing, G. W. Simon, "Charged Particle Radiation Damage in Semiconductors, III: The Energy Dependence of Proton Damage in Silicon," Contract NAS5-1851, 8653-6005-KU-000, 4 October 1962.

3. J. M. Denney, R. G. Downing, G. W. Simon, "Energy Dependence of Proton Damage in Silicon," Physical Review, 129, No. 6, 2454, (1963).

4. J. M. Denney, R. G. Downing, M. E. Kirkpatrick, G. W. Simon, W. K. Van Atta, "Charged Particle Radiation Damage in Semiconductors, IV: High Energy Proton Radiation Damage in Solar Cells," Contract NAS5-1851, 8653-6017-KU-000, 20 January 1963.

5. J. R. Carter, R. G. Downing, "Charged Particle Radiation Damage in Semiconductors, VII: Energy Levels of Defect Centers in Electron and Proton Bombarded Silicon," Contract NAS5-1851, 8653-6021-KU-000, 15 February 1963.